

## A STUDY OF RUNAWAY GENERATION IN THE ISTTOK TOKAMAK.

V.V.Plyusnin\*, J.A.C.Cabral, H.Figueiredo, C.A.F.Varandas, I.S.Nedzel'skij.

*Centro de Fusão Nuclear, Association Euratom/IST, Instituto Superior Técnico,  
Av. Rovisco Pais, 1049 – 001 Lisboa PORTUGAL*

### 1. Introduction.

Runaway generation is one of the fundamental physical processes in plasmas being under the action of external electric fields. Usually, the runaways occur in discharges with low density plasmas and relatively high longitudinal electric fields applied. This phenomenon has been intensively studied both experimentally and theoretically (as, for example, [1-4]). Such studies are still actual, because the creation of runaways in disruptions or during fast current ramp-down in reactor-scale tokamaks will lead to unacceptable electromechanical and thermal stresses [5].

Anomalously low plasma resistivity and ion heating are the first experimental evidences of runaways. The analysis of X-ray emission, ECE radiation and measurements performed with the Thomson scattering diagnostic allow to describe quantitatively the runaway process [3,4]. The synchrotron radiation has been detected in TEXTOR-94 with an infrared camera for the direct observation of the runaway beam image [6].

This paper presents the results of a runaway generation study carried out on the ISTTOK tokamak ( $R_0=0.46$  m,  $a_{pl}\leq 0.085$  m,  $B_0\leq 0.5$  T) [7]. The runaway-related events, including typical relaxation phenomena were observed in discharges with current density values  $\langle j_{pl} \rangle \cong 0.2-0.5$  MA/m<sup>2</sup> in the plasma density range  $(1-5)\cdot 10^{18}$  m<sup>-3</sup>. Since the diagnostics based on the analysis of radiation from plasmas (X-ray emission, ECE radiation, Thomson scattering) were not available in this study, the runaway process was investigated by the analysis of macroscopic plasma parameters carried out in the frame of runaway theory and numerical modelling. All considerations were carried out in zero-dimensional approximation.

### 2. Analysis of parameters and detection of runaway regimes.

Due to the high  $E_0$  values ( $E_0\sim 8-10$  V/m) applied for discharge creation, the criterion  $E_0/p_0 > (2-2.5)\cdot 10^4$  V/m $\cdot$ torr<sup>-1</sup>, where  $p_0$  is the value of the working gas pressure, taken as the threshold condition for runaway regime on the break-down stage [8], was exceeded in experiments and in some cases after initial break-down the further discharge development was not possible. Therefore, despite of inevitable intensive losses [1,3] a significant runaway production at the earlier stage of discharge can be expected in the ISTTOK experiments.

Another criterion of runaway conditions which can be written in the following form  $K \equiv 10^{19} \langle j_{pl} \rangle [A/m^2] / (1.4 \times 10^6 \langle n_e \rangle [m^{-3}]) \geq 1$  was established in multiple earlier investigations on tokamaks [1,4]. This criterion directly underlines the runaway character of the discharge and can be easily evaluated from the measurements of macroscopic plasma parameters  $I_{pl}$  and  $\langle n_e \rangle$ . The runaway regimes detected in ISTTOK (Fig.1) have the features similar to those commonly observed in runaway tokamak experiments [1,3,4,9]. The increase of plasma current with simultaneous drops in loop voltage and MHD activity were preceded by the plasma density decrease below the critical value determined from the condition  $K=1$ . Usually, the decrease of MHD activity is the consequence of a significant runaway fraction in the total plasma current. The runaway criterion was satisfied for a large amount of obtained experimental data mainly due to the low plasma density at relatively high plasma currents ( $q(a) \sim 3-4$ ). The formation of noticeable current plateau at  $t \cong 500-700$   $\mu$ s after discharge termination which was observed in some shots also should be addressed to the presence of runaways [1,6,9,10].

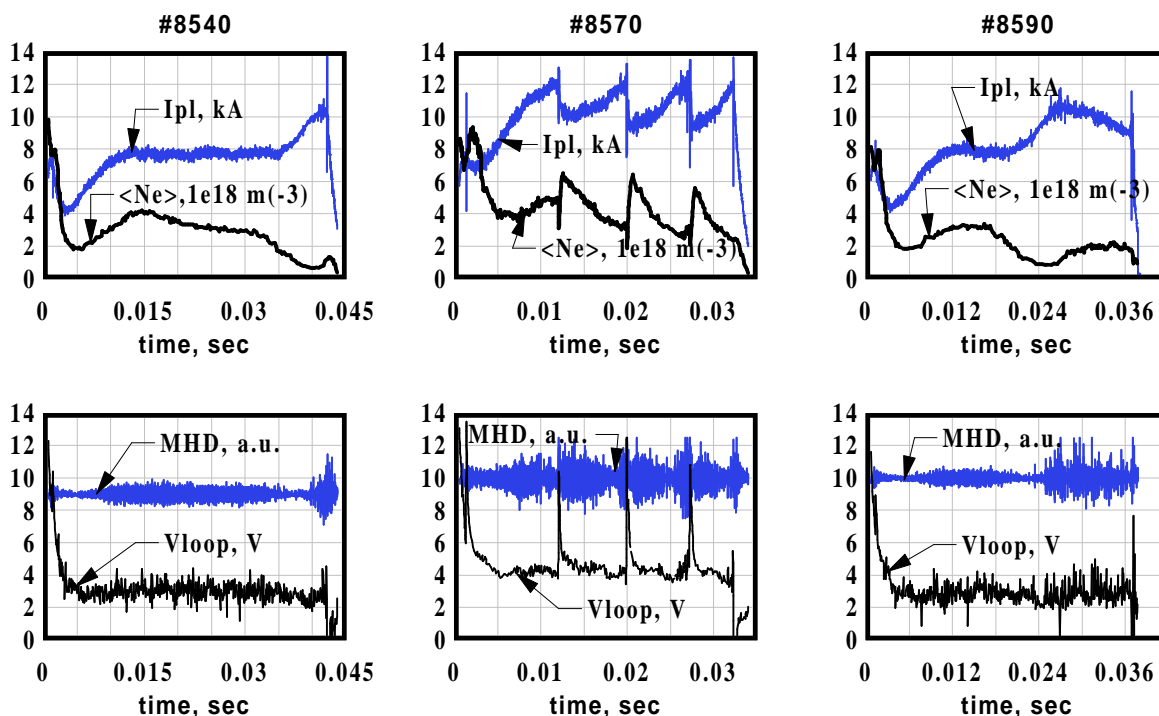


FIG.1. The time traces of the plasma parameters in discharges with runaway generation events.

It is well known that runaway electrons, due to their highly anisotropic distribution function, can be a source of plasma instabilities [1,4,11,12] and, in turn, the development of some instabilities in tokamak discharge enables the runaway generation. The disruptive instability is an example of instability which leads to the creation of runaways together with enhanced impurity release and plasma cooling [13]. The disruptive-like events (DLE) in shot

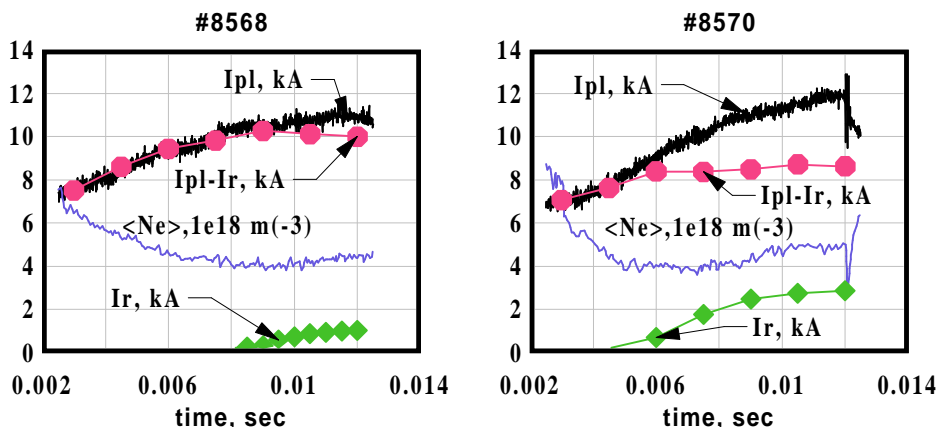


FIG.2. The effect of the runaway currents on the achievement of DLE conditions.

#8570 occurred at  $q(a) \approx 3.2$  (Figs.1,2). In shot #8568 (Fig.2), at the same  $V_{loop}$  and  $B_{vert}$  values, the plasma current was  $\sim 7-10\%$  less and the DLE condition was not achieved. After DLEs a significant density decrease enabled the runaway process, which resulted in a voltage drop with simultaneous current increase till the next DLE started. Note, that the incremental increase of MHD activity and oscillations in  $V_{loop}$  signal and correlation between bursts of oscillations in both signals are clearly seen and preceded to the 2<sup>nd</sup> and the 3<sup>rd</sup> DLEs. The relaxations are seen also in  $I_{pl}$  signal before the 3<sup>rd</sup> DLE (Fig.3). The observed phenomena are very similar to those detected in tokamak discharges with instability driven by runaway electrons [1,3,4,11].

### 3. Results on runaway current evaluation and discussion.

The runaway process is very sensitive to the electron temperature and density. Since independent measurements of  $T_e$  were not available, the calculation of the runaway current ( $I_r$ ) from the experimental data was carried out taking into account the results of numerical modelling. In this modelling the evolution of the discharge parameters was simulated including the effect of runaway generation. It was done in the frame of 0-D model which includes the equations of energy balance for electrons, ions and atoms as well as particle balance equations with characteristic confinement times evaluated as  $\tau_e \cong (1-4)10^{-4}$  sec [14]. This set of equations was completed by the equations of electric circuit for capacitor battery driven discharge in equivalent 'perfect transformer' scheme and by an equation of evolution of runaway electron density for calculation of  $I_r$  in the continuous creation model [9]. The following equations were used in the modelling:

$$\begin{aligned} dV_{loop}/dt &= -(I_{pl} + I_r) / C & d(n_a T_a)/dt &= P_{cx} - P_{convection\_loss} \\ dI_{pl}/dt &= (V_{loop} - I_{pl} * R_{pl}) / L_{pl} - dI_r / dt & dn_e / dt &= n_e n_a * \langle \sigma v \rangle_{ion} - n_e / \tau_p \\ d(n_e T_e)/dt &= P_{OH} - P_{loss} - n_e T_e / \tau_{Ee} & dn_a / dt &= - n_e / dt \\ d(n_i T_i)/dt &= P_{ei} - P_{cx} - n_i T_i / \tau_{Ei} & dn_r / dt &= \lambda_r - n_r / \tau_r \end{aligned}$$

The runaway current was calculated as  $I_r = \pi a^2 e n_r c A_0 * ((ec/m_e)^2 + A_0^2)^{-1/2}$  in numerical modelling and evaluated as  $I_r = \int \pi a^2 e \lambda_r c A_0 * ((ec/m_e)^2 + A_0^2)^{-1/2} dt$  from the experimental data, where  $\lambda_r \cong \text{const}(Z_{eff})(E_{cr}/E_0)^{3(Z+1)/16} n_e v_e \exp\{-E_{cr}/4E_0 - \text{sqrt}((Z+1)E_{cr}/E_0)\}$  is the runaway particle flux given by [2] and  $A_0 = \int E_0 dt$  - the vector potential of the poloidal magnetic field.

The numerical modelling allowed to estimate the reasonable limits of such plasma parameters as electron temperature  $\langle T_e \rangle \sim 30-70$  eV,  $Z_{eff} \sim 2-3$  and  $I_r \sim 1-5$  kA at other macroscopic parameters being chosen close to the experimental ones. These  $\langle T_e \rangle$  and  $Z_{eff}$  values were used as a starting point in calculations of  $I_r$  from the experimental data. The modified Ohm's law:  $E_0(t) = E_0(1 - I_r(t)/I_{total}(t))$  and usual formula of the Spitzer's resistivity:  $\eta_{pl} = \text{Const} * Z_{eff} * f(Z_{eff}) * \ln \Lambda * T_e^{-3/2}$  were used to update in calculations the actual values of  $I_r$  and  $\langle T_e \rangle$  according to the changes in the Ohmic heating power and other plasma parameters.

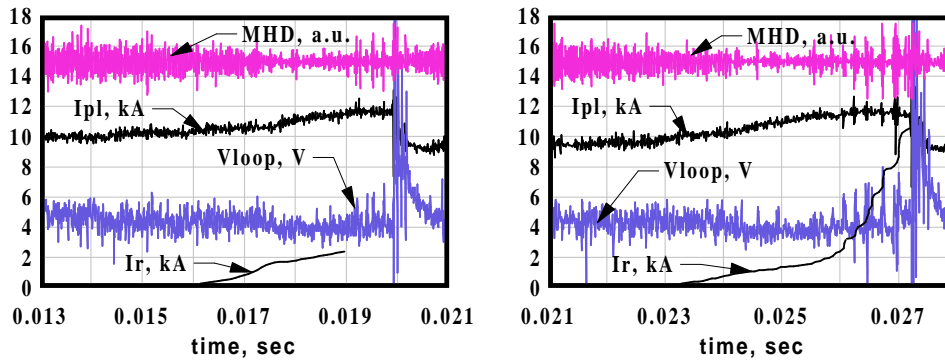


FIG.3. Shot #8570. The evolution of plasma parameters and runaway currents between DLEs.

The best matching of the calculated runaway current to the evolution of macroscopic plasma parameters is found to be at  $\langle T_e \rangle = 40$  eV and  $Z_{eff} = 2$  before the 1<sup>st</sup> DLE in #8570 and in the same time range in #8568 (without DLE) (Fig.2). It is seen that a higher value of the total plasma current which led to DLEs in #8570 is associated with a higher value of  $I_r$ . Such a result can be explained by slightly lower plasma density in #8570 in comparison to #8568, since  $E_{cr} \sim n_e / T_e$  in the expression for  $\lambda_r$ . During the transient stage of DLE the plasma parameters strongly changed in a very short time:  $\Delta I_{pl} \sim 20\%$ ,  $\Delta V_{loop} \cong \pm 10V$ ,  $\Delta \langle n_e \rangle \cong \pm 50\%$  of the

initial value. It is assumed that during instability event the runaway current completely disappears and the process of substitution of the plasma resistive current by the current of runaways [15] is insignificant. That is why the calculation of the runaway current was carried out only during stages between DLEs where the plasma parameters varied slowly. After the 1<sup>st</sup> and further DLEs the electron temperature slightly decreased, which can be explained by the enhanced impurity release during DLEs.

The analysis of the behaviour of the calculated  $I_r$  in latter cases (i.e after the 1<sup>st</sup> DLE) in comparison to the evolution of measured  $I_{pl}$  yields, however, a significant difference in evolutions just before DLEs. The saturation in  $I_{pl}$  clearly correlates with the incremental appearance of  $V_{loop}$  and MHD bursts, while the continuous creation model yields the step-like  $I_r$  increase (Fig.3). Qualitatively such a difference can be explained by the appearance of an instability driven by the runaway electrons (fan instability) [4,11,12]. This instability tends to isotropize the runaway beam in the velocity space. It appears when the runaway electron beam velocity exceeds the critical value:  $V_{beam} > 3V_{Te}(E_{cr}/E_0)^{1/2}(\omega_{ce}/\omega_{pe})^{3/2}$  [3,4,11,12]. According to the theory of this instability [11,12] the bursts of  $V_{loop}$  are the evidence for the retardation effect of the runaway electron beam. The similar saturation of the plasma current under runaway conditions is clearly seen also in shots #8540 and #8590.

A simple evaluation shows that at the given experimental parameters ( $\langle n_e \rangle$ ,  $V_{loop}$ ) and  $\langle T_e \rangle \sim 40$  eV the fan instability condition  $V_{beam}/V_{Te} \sim 10$  can easily be achieved. At the values  $I_r \sim 3$  kA and  $V_{beam} \sim 10 V_{Te}$  the density of runaway electrons is varied in a range of two orders of magnitude depending on the beam radius:  $2.5 \cdot 10^{16} [m^{-3}] < n_r < 1.5 \cdot 10^{18} [m^{-3}]$ .

#### 4. Summary.

The runaway regimes were identified in the majority of the discharges in the ISTTOK tokamak. Their characteristic feature is that the runaway electron current is a significant part of the total plasma current. It leads in some cases to the appearance of disruptive-like events due to the temporal loss of equilibrium and stability.

The runaway beam instability was observed in the experiments. This instability led to saturation of the plasma current own by the retardation effect of the runaway fraction in the total current.

#### References.

- [1] H. Knoepfel, D.A. Spong, Nuclear Fusion, 19 (1979) 785.
- [2] R.H. Cohen. Physics of Fluids, 19 (1976) 239
- [3] H. de Kluiver, N.F. Perepelkin, A. Hirose. Experimental Results on Current Driven Turbulence in Plasmas – A Survey. Physics Report, Vol.199, no.6, January 1991.
- [4] V.V. Alikaev, K.A. Razumova, Yu.A. Sokolov. Plasma Physics Reports, 1 (1975) 303
- [5] M.N. Rosenbluth et al. Proc. of the 16<sup>th</sup> International Conference on Fusion Energy, Montreal, 1996, IAEA, Vienna 1997, Vol.2, 979-986.
- [6] I.M. Pankratov et al. 26<sup>th</sup> EPS Conference on CFPP, Maastricht, ECA (1999) Vol.23J, 597.
- [7] J.A.C. Cabral et al. Plasma Physics and Controlled Fusion. 38(1996)51
- [8] B. Lloyd, et al. Nuclear Fusion, 31(1991)2031
- [9] D.W. Swain, S.J. Zweben. Nuclear Fusion 20(1980)711
- [10] V.V. Plyusnin et al. In: A Collection of Papers Presented at the IAEA TCM on Research Using Small Fusion Devices. Chengdu, P. R. China, 1999. Report P8. (to be published)
- [11] V.V. Parail, O.P. Pogutse. Nuclear Fusion, 18(1978)303,
- [12] V.V. Parail, O.P. Pogutse. Nuclear Fusion, 18(1978)1357
- [13] J. Wesson et al. Nuclear Fusion, 29(1989)641
- [14] J. Wesson. TOKAMAKS. Clarendon Press, Oxford, 1997
- [15] R. Jaspers et al. Nuclear Fusion. 36(1996)367

\*- e-mail: vlad@cfm.ist.utl.pt

Fax: +351 1 8417819

permanent affiliation:

Institute of Plasma Physics NSC KIPT Kharkov, UKRAINE